Biochem. J. (1992) 283, 223–233 (Printed in Great Britain)

Mechanism of D-fructose isomerization by *Arthrobacter* D-xylose isomerase

Minnie RANGARAJAN and Brian S. HARTLEY*
Centre for Biotechnology, Imperial College of Science, Technology and Medicine, London SW7 2AZ, U.K.

The mechanism of D-fructose isomerization by *Arthrobacter* D-xylose isomerase suggested from X-ray-crystallographic studies was tested by detailed kinetic analysis of the enzyme with various metal ions at different pH values and temperatures. At D-fructose concentrations used in commercial processes Mg^{2+} is the best activator with an apparent dissociation constant of 63 μM; Co^{2+} and Mn^{2+} bind more strongly (apparent K_d 20 μM and 10 μM respectively) but give less activity (45% and 8% respectively). Ca^{2+} is a strict competitive inhibitor versus Mg^{2+} (K_i 3 μM) or Co^{2+} (K_i 105 μM). The kinetics show a compulsory order of binding; Co^{2+} binds first to Site 2 and then to Site 1; then D-fructose binds at Site 1. At normal concentrations Mg^{2+} binds at Site 1, then D-fructose and then Mg^{2+} at Site 2. At very high Mg^{2+} concentrations (> 10 mM) the order is Mg^{2+} at Site 1, Mg^{2+} at Site 2, then D-fructose. The turnover rate ($k_{cat.}$) is controlled by ionization of a residue with apparent pK_a at 30 °C of 6.0 ± 0.07 (Mg^{2+}) or 5.3 ± 0.08 (Co^{2+}) and ΔH = 23.5 kJ/mol. This appears to be His-219, which is co-ordinated to M[2]; protonation destroys isomerization by displacing M[2]; Co^{2+} binds more strongly at Site 2 than Mg^{2+}, so competes more strongly against H^+. The inhibition constant (K_i) for the two competitive inhibitors 5-thio-α-D-glucopyranose and D-sorbitol is invariant with pH, but $K_{m(app.)}$ in the Mg[1]-enzyme is controlled by ionization of a group with pK_a 6.8 ± 0.07 and ΔH = 27 kJ/mol, which appears to be His-53. This shows that $K_{m(app.)}$ is a complex constant that includes the rate of the ring-opening step catalysed by His-53, which explains the pH-dependence. In the Mg[1]Mg[2]-enzyme or Co[1]Co[2]-enzyme, the pK_a is lower (6.2 ± 0.1 or 5.6 ± 0.08) because of the extra adjacent cation. Hence the results fit the previously proposed pathway, but show that the mechanisms differ for Mg^{2+} and Co^{2+} and that the rate-limiting step is isomerization and not ring-opening as previously postulated.

INTRODUCTION

Elucidation of the catalytic mechanism of *Arthrobacter* D-xylose isomerase enzyme is important, not only for scientific reasons, but as a guide to improvements that might be made by protein engineering to improve its properties as a commercial glucose isomerase for production of high-fructose syrups. As part of this programme, the basic properties of the enzyme (Smith *et al.*, 1991), the cloning and expression of the structural gene in either *Arthrobacter* or *Escherichia coli* hosts (Loviny-Anderton *et al.*, 1991) and tertiary structure of the Mg^{2+}–enzyme–xylitol complex at 0.23 nm (2.3 Å) and Mg^{2+}–enzyme–sorbitol complex at 0.25 nm (2.5 Å) resolution (Henrick *et al.*, 1989) have been reported.

Tertiary structures of the enzyme with various bound inhibitors or metal ions led to the hypothesis of a rather surprising mechanism for glucose–fructose isomerization, involving two adjacent bivalent metal ion sites (Collyer *et al.*, 1990). This has the following steps as illustrated in Fig. 1 (Collyer *et al.*, 1990).

(i) Binding of the α-D-pyranose form of the glucose or xylose substrates, so that O-3 and O-4 co-ordinate to a bivalent metal ion at Site 1 that is also co-ordinated to Glu-180, Glu-216, Asp-244 and Asp-292. This orients the substrate so that the C-1 hydroxy group can form a hydrogen bond to His-53, which is also hydrogen-bonded to a buried Asp-56.

(ii) Ring-opening catalysed by this 'charge-relay system', analogous to that in chymotrypsin (Blow *et al.*, 1969), in which the C-1 hydroxy-group hydrogen atom transfers to O-5. Collyer *et al.* (1990) argue that this step is rate-limiting in the overall isomerization process.

(iii) Chain extension to a position in which O-2 and O-4 now co-ordinate to M[1]. This is seen in crystals soaked in substrates. The metal ion at Site 2 (co-ordinated to Glu-216, His-219, Asp-254 and Asp-256) is not at this stage in direct contact with the substrate.

(iv) Isomerization via an anionic transition state arising from translocation of M[2] to an adjacent Site 2′ in which it co-ordinates to O-1 and O-2 of the substrate together with M[1] (to O-2). The constellation of positive charge, assisted by hydrogen-bonding to O-1 of the protonated amino group of Lys-182, induces a symmetrical C-1/C-2 transition state in which a hydride ion is situated midway between C-1 and C-2. The shielding of this hydride ion from solvent, provided by Phe-93, Trp-136 and Phe-25′ of an adjacent subunit, is an essential feature of this transition state.

The remaining steps are formally the reverse of steps (i) to (iv), as follows.

(v) Collapse of the transition state, by return of M[2′] to Site 2.

(vi) Chain contraction to a pseudocyclic position with ligands to M[1] changing from O-2/O-4 back to O-3/O-4.

(vii) Ring-closure, catalysed by His-53, yields α-D-fructofuranose.

(viii) The α-D-fructofuranose leaves but the two metal ions remain.

The present paper describes a detailed study of the kinetics of the enzyme with various metal ions at various pH values, designed to test this hypothesis. The results support it in principle, but suggest that the pathway is different for the Mg^{2+}- and Co^{2+}-enzymes. Moreover the rate-limiting step appears to be isomerization, and not ring-opening as postulated.

MATERIALS AND METHODS

Unless otherwise stated, all materials and methods were as in Smith *et al.* (1991).

D-Xylose isomerase

The Mg^{2+}-enzyme was purified from *Arthrobacter* N.R.R.L.

* To whom correspondence should be addressed.

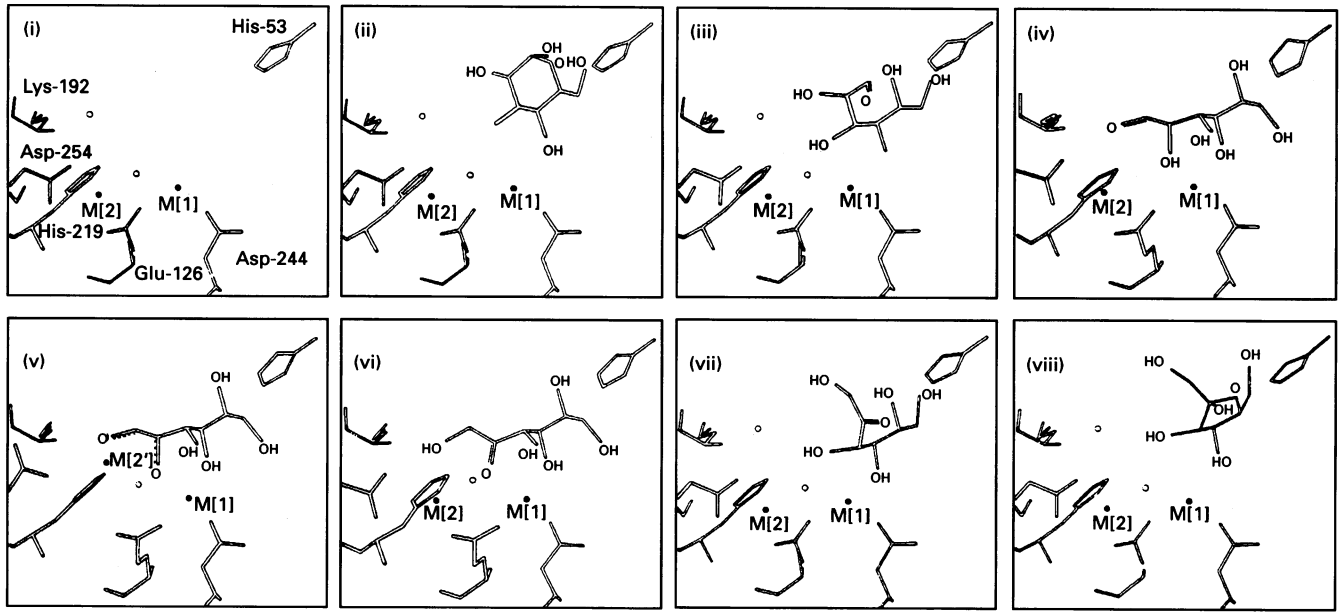

Fig. 1. Mechanism of isomerization by D-xylose isomerase

Reproduced by courtesy of Collyer *et al.* (1990).

B3728 as described previously. The apoenzyme was prepared by dialysing this exhaustively at 4 °C versus 0.01 M-EDTA (disodium salt)/0.1 mM-phenylmethanesulphonyl fluoride/0.05 M-Tris/HCl buffer, pH 7.5, and then against the same mixture lacking EDTA. The Co^{2+}-enzyme and Mn^{2+}-enzyme were prepared by incubating the apoenzyme with 5 mM-$CoCl_2$ or 5 mM-$MnCl_2$ at 30 °C overnight.

Enzyme assays

Kinetic studies of the rate of formation of D-glucose from D-fructose were by a colorimetric GOD–PERID assay kit (BCL, Lewes, East Sussex, U.K.) containing glucose oxidase, peroxidase and diammonium 2,2′-azinobis-(3-ethylbenzothiazoline-6-sulphonate as described by Smith *et al.* (1991). Although the product of the isomerase reaction is α-D-glucose, and glucose oxidase is specific for β-D-glucopyranose (Duke *et al.*, 1969), the assay is valid since the catalytic constant for the mutarotation of D-glucose at 25°C in acid is 4.5×10^{-3} s^{-1} (Isbell & Pigman, 1969), giving a $t_{\frac{1}{2}}$ of 2.6 min. Therefore, in 15% (w/v) trichloroacetic acid, any α-D-glucose formed by isomerization of D-fructose will rapidly be in equilibrium with the β-anomer.

Buffers used were acetate, Caps [3-(cyclohexylamino)-1-propanesulphonic acid], Hepes, Mes, Mops and Tris/HCl. Unless otherwise specified, all buffers were adjusted to ionic strength of 9.5 mS by addition of NaCl. pH adjustments were made with a Radiometer 26 pH-meter at room temperature; the actual pH at the temperature of the experiment was calculated from heats of ionization of the buffers: $\Delta pH/°C = -0.011$ for Mes, -0.013 for Mops, -0.014 for Hepes and -0.028 for Tris/HCl (Good *et al.*, 1966).

Assay solutions (1 ml), generally containing D-fructose and 10 mM-Mg^{2+} or 2 mM-Co^{2+} or 2 mM-Mn^{2+} in 0.1 M buffers, were preincubated for 45 min in a water bath regulated by a Braun Thermomix B regulator. Reaction was initiated by adding enzyme (15–200 μg as appropriate for pH and temperature) in 20 μl of the same buffer. Portions (100 μl) were added at suitable time intervals to 100 μl of 15% (w/v) trichloroacetic acid to stop the reaction, and then 5 ml of GOD–PERID reagent in 0.1 M-phosphate buffer, pH 7.0, was added. The absorbance at 610 nm, with the use of a reagent blank, was measured after 25 min at room temperature. The glucose formed was calculated from a calibration curve; initial velocities (always linear) are expressed as units/mg of enzyme, where 1 unit is defined as 1 μmol of glucose formed/min.

D-Xylose isomerase assays used the NADH-linked arabitol dehydrogenase assay method of Smith *et al.* (1991). Assay solutions (1 ml containing 0.1 M-D-xylose, 0.33 mM-NADH, 30 mM-Mg^{2+}, 0.1 M-Tris/HCl buffer, pH 8.0, and 1 unit of arabitol dehydrogenase) were preincubated at 30 °C in plastic disposable cuvettes in a Cary recording spectrophotometer. Reaction was initiated by adding enzyme (5–10 μg in 50 μl) and the decrease in absorbance at 340 nm was measured. One unit of xylose isomerase activity is the amount of enzyme that converts 1 μmol of D-xylose into D-xylulose in 1 min.

Enzyme kinetics

Values of maximum velocity ($V_{max.}$) and apparent K_m were derived by non-linear-regression analysis of the data using the ENZFITTER Data Analysis Program (Robin J. Leatherbarrow) published by Biosoft (Cambridge, U.K.) with 0.04–3 M-D-fructose at 30.0±0.1 °C. To determine K_i of inhibitors at any given pH by using Dixon plots (Dixon & Webb, 1964, pp. 63–70), three or four concentrations of fructose and five different concentrations of inhibitor (0–25 mM for D-sorbitol and 0–50 mM for 5-thio-D-glucose) were used. To determine the enthalpy of ionization, measurements were made in the temperature range 25–50 °C.

Reversibility of the effect of pH on rate over the assay periods was assured by reassaying the enzyme after readjusting the pH to 7.5. Possible dependence of reaction rates on the concentration and type of buffer was eliminated by varying these, keeping the ionic strength constant: acetate, Mes, Mops, Hepes and Caps did not show any interference.

For simple measurements of maximum velocities of Mg^{2+}-xylose isomerase, 3.2 M-D-fructose was used, which is at least 15-fold the $K_{m(app.)}$ at pH > 6.70. At lower pH, the substrate concentration was at least 4-fold in excess of the $K_{m(app.)}$. Values of $V_{max.}$ obtained in this way were corrected for any variation in $K_{m(app.)}$. For the Co^{2+}- and Mn^{2+}-enzymes, values for $V_{max.}$ were calculated from $K_{m(app.)}$ values determined from non-linear-

regression analysis because maximum fructose solubility is insufficiently in excess of $K_{m(app.)}$ at all pH values.

Reconstitution of holoenzymes

To ensure correct > 99% reconstitution, apoenzyme (0.75 mg/ml) was incubated at 4 °C or 30 °C in 0.05 M-Tris/HCl buffers containing 30 mM-Mg^{2+} or 5 mM-Co^{2+} at pH 8.0 or pH 7.0 respectively (adjusted to compensate for temperature). Samples of enzyme were removed at different times and assayed immediately against D-xylose at 30 °C. Over 4 h at 30 °C or 20 h at 4 °C was found to be necessary for 99% reconstitution as measured by specific activity of the reconstituted enzyme compared with the specific activity of enzyme purified in the presence of Mg^{2+}, and holoenzymes were routinely prepared under these conditions.

Effects of bivalent metal ions on enzyme activity

Duplicate samples of apoenzyme (0.4 mg/ml) in 0.05 M-Tris/HCl buffer, pH 7.0, containing from 1 μM to 20 mM-Mg^{2+}, -Co^{2+} or -Mn^{2+}, were incubated in 1 ml plastic tubes at 30°C for 5 h. The D-fructose (1 M) and D-xylose (0.1 M) activities were assayed at the same M^{2+} concentration. The Co^{2+} or Mn^{2+} activities were calculated as a percentage of the activity obtained with Mg^{2+}.

The effect of a mixture of Mg^{2+} and Co^{2+} on isomerase activity was determined by preincubating apoenzyme (2.5 mg/ml) at 30 °C for 20 h in 0.1 M-Mops buffer, pH 7.90, containing either 10 mM-Mg^{2+} or 2 mM-Co^{2+} or both, and assaying versus D-fructose (1.5 M and 4 M) in similar buffers at 30 °C.

The inhibition constant (K_i) for Ca^{2+} for the Mg^{2+}-enzyme was determined by preincubating apoenzyme (0.4 mg/ml) in 0.05 M-Tris/HCl buffer, pH 8.0, containing Mg^{2+} (0.05–50 mM) plus or minus Ca^{2+} (12.5, 25 or 50 μM) in 1 ml plastic tubes at 30 °C for 20 h. Activity versus 1.5 M-D-fructose in similar cation mixtures was assayed. K_i was calculated from Lineweaver–Burk plots of $1/v$ versus $1/[Mg^{2+}]$ at each value of $[Ca^{2+}]$.

The K_i of Ca^{2+} for the Co^{2+}-enzyme was determined in the same way, using Co^{2+} concentrations (0.005–2 mM), plus or minus Ca^{2+} (50, 200 or 500 μM), and assayed against 3 M-fructose in similar solutions.

Kinetic analysis of order of ligand binding

Apoenzyme was preincubated at 30 °C for 20 h with Mg^{2+} (0.1–10 mM) in 0.1 M-Mops buffer, pH 7.90, or with Co^{2+} (0.005–2 mM) in 0.1 M-Mops buffer, pH 7. Initial velocities were measured in similar solutions containing 0.04–1.5 M-D-fructose for the Mg^{2+}-enzyme or 0.4–3 M-D-fructose for the Co^{2+}-enzyme. Another series of experiments used 0.2–2 M-D-fructose and Mg^{2+} over a range 0.1–10 mM.

The kinetic analysis described by Dixon & Webb (1964, pp. 420–443) allows determination of order of ligand binding for a single activator metal ion in a simple Michaelis–Menten enzyme reaction. The mechanism proposed by Collyer *et al.* (1990) involves two metal ions and two consecutive catalytic steps, but the evidence discussed below suggests that the rate-limiting step (k) is not ring-opening but isomerization. Hence the approach of Dixon & Webb (1964, pp. 420–443) was extended to this case as follows.

Scheme 1. The mechanism proposed by Collyer *et al.* (1990) also assumes that substrate, α-D-fructofuranose (F_f) in our case, binds only to enzyme (E) in which metal ions are already bound at Site 1 (M_1) and Site 2 (M_2). Co^{2+} binds most strongly at Site 2 (see below) so we can express this case as shown in Scheme 1, where K_2, K_1 and K_F' are dissociation constants of the metal ions and fructose from their respective complexes, but K_O' is a complex constant representing the equilibrium between the bound fructofuranose form and the extended-chain form (F_O). This will apply if the forward and backward rates for ring-opening and chain extension are much faster than the isomerization rate (k). These assumptions appear to be justified, so we can use either Michaelis–Menten kinetics or steady-state kinetics to yield the following equations:

$$v = \frac{V_{max.}[S]}{[S]+K_{m(app.)}} = \frac{k[E][S]/(1+K_O')}{[S]+K_m(1+K_1/[M])}$$

where

$$V_{max.} = \frac{k[E]}{(1+K_O')} \text{ and } K_m = \frac{K_F'K_O'}{(1+K_O')} \quad (1)$$

$V_{max.}$ and $K_{m(app.)}$ are experimentally determined values. K_m is the value of $K_{m(app.)}$ at saturating metal ion concentration and K_1, K_2 and K_F' are simple dissociation constants for the two metal ions and fructose from their respective complexes. Note, however, that K_O' is a complex constant that includes the kinetics of the ring-opening and chain-extension steps.

For experiments conducted at constant [M] and variable [S], Lineweaver–Burk plots of $1/v$ versus $1/[S]$ give straight lines from which values of $K_{m(app.)}$ and $V_{max.}$ can be determined:

$$\frac{1}{v} = \frac{1}{V_{max.}} + \frac{K_{m(app.)}}{V_{max.}} \times \frac{1}{[S]} \quad (2)$$

$V_{max.}$ is independent of the concentration of the activator metal ion, and plots of $K_{m(app.)}$ versus $1/[M]$ yield straight lines of intercept K_m and slope K_mK_1 from which both these constants can be determined.

For experiments conducted at constant [S] and variable [M], plots of $1/v$ versus $1/[M]$ also give straight lines from which apparent values of $V_{max.}$ and $K_{m(app.)}$ can be determined:

$$\frac{1}{v} = \frac{1}{V_{max.}} + \frac{K}{V_{max.}} \times \frac{1}{[M]}$$

where

$$\frac{1}{V_{max.}} = \frac{(1+K_O')}{k[E]} + \frac{K_F'K_O'}{k[E]} \times \frac{1}{[S]} \text{ and } \frac{1}{K} = \frac{1}{K_1} + \frac{[S]}{K_1K_m} \quad (3)$$

A secondary plot of $1/V_{max.}$ versus $1/[S]$ has intercept = $(1+K_O')/k[E]$, and slope = $K_F'K_O'/k[E]$, and a secondary plot of $1/K$ versus [S] gives intercept = $1/K_1$ and slope = $1/K_1K_m$, allowing all these constants to be determined.

Scheme 2. This envisages an alternative mechanism in which the holoenzyme contains only one strongly bound metal ion at Site 1, to which the substrate binds as observed in the structure proposed by Henrick *et al.* (1989) for the Mg^{2+}–xylitol–enzyme complex. Only then does a second metal ion bind at Site 2 (Scheme 2).

In this case, Michaelis–Menten kinetics yields the following equation:

$$v = \frac{V_{max.}[S]}{[S]+K_{m(app.)}}$$

where

$$V_{max.} = \frac{k[E][M]}{[M]+K_2(1+K_O)} \text{ and } K_{m(app.)} = \frac{K_2K_FK_O(1+K_1/[M])}{[M]+K_2(1+K_O)} \quad (4)$$

$$E + M \overset{K_2}{\rightleftharpoons} EM_2 + M \overset{K_1}{\rightleftharpoons} EM_1M_2 + F_f \overset{K_F'}{\rightleftharpoons} EM_1M_2 - F_f \overset{K_O'}{\rightleftharpoons} EM_1M_2 - F_O \xrightarrow{k} EM_1M_2 - G_p$$

Scheme 1.

$$E + M \overset{K_1}{\rightleftharpoons} EM_1 + F_f \overset{K_F}{\rightleftharpoons} EM_1 - F_f \overset{K_O}{\rightleftharpoons} EM_1 - F_O + M \overset{K_2}{\rightleftharpoons} EM_1M_2 - F_O \overset{k}{\longrightarrow} EM_1 + M + G_p$$

Scheme 2.

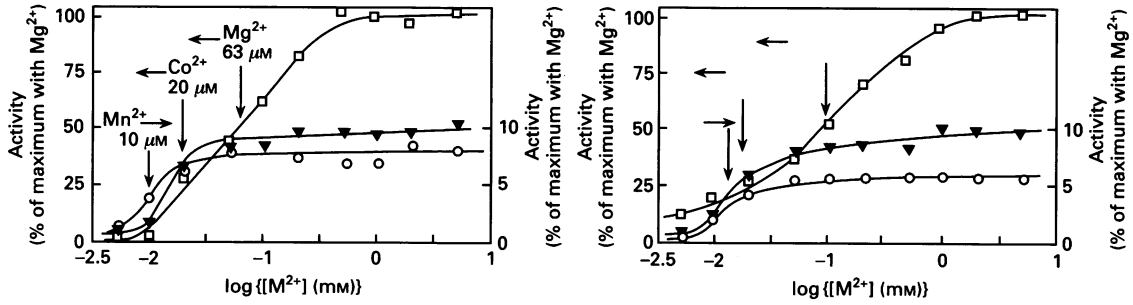

Fig. 2. Effect of bivalent cations on isomerase activity

Apoenzyme (0.4 mg/ml) was preincubated at 30 °C for 5 h in 0.05 M-Tris/HCl buffer, pH 7.0, containing 10 μM–20 mM-Mg^{2+} (□; left-hand scale), -Co^{2+} (▼; left-hand scale) or -Mn^{2+} (○; right-hand scale) and then assayed against (*a*) 1.0 M-D-fructose or (*b*) 0.1 M-D-xylose, in similar buffers. Activities with each substrate are expressed as percentages of the maximum activity obtained with Mg^{2+}.

For experiments conducted at constant [M] and variable [S], Lineweaver–Burk plots of $1/v$ versus $1/[S]$ give straight lines from which apparent values of K_m and $V_{max.}$ can be determined. However, $V_{max.}$ is dependent on the concentration of the activator metal ion, and:

$$\frac{1}{V_{max.}} = \frac{1}{k[E]} + \frac{K_2(1+K_O)}{k[E]} \times \frac{1}{[M]} \quad (5)$$

Hence plotting $1/V_{max.}$ versus $1/[M]$ gives a straight line of intercept $1/k[E]$ and negative intercept $1/K_2(1+K_O)$ on the respective axes. The dependence of $K_{m(app.)}$ on metal ion concentration is more complex, since:

$$K_{m(app.)}\{[M] + K_2(1+K_O)\} = K_2K_FK_O(1+K_1/[M])$$

However, at high concentrations of activator ion, where $[M] \gg K_2$, as in the experiments reported below, this reduces to:

$$K_{m(app.)} = K_2K_FK_O \times \frac{1}{[M]} + K_1K_2K_FK_O \times \frac{1}{[M]^2} \quad (6)$$

so that plots of $K_{m(app.)}$ versus $1/[M]$ approximate to straight lines where terms in $1/[M]^2$ can be ignored. Since $K_2(1+K_O)$ was determined from eqn. (5), $K_m = K_OK_F/(1+K_O)$ can then be calculated.

Plotting $K_{m(app.)}/V_{max.}$ versus $1/[M]$ gives a parabolic plot from which K_1 can be determined:

$$\frac{K_{m(app.)}}{V_{max.}} = \frac{K_2K_FK_O(1+K_1/[M])}{k[E]} \times \frac{1}{[M]} \quad (7)$$

Alternatively, for experiments conducted at constant [S] and variable [M], eqn. (4) can be rearranged to give:

$$\frac{1}{v} = \frac{1}{k[E]} + \frac{K_2(1+K_O)([S]+K_m)}{k[E][S]} \times \frac{1}{[M]} + \frac{K_1K_2K_FK_O}{k[E][S]} \times \frac{1}{[M]^2} \quad (8)$$

Plotting $1/v$ versus $1/[M]$ gives parabolic plots of the form $1/v = a + b(1/[M]) + c(1/[M])^2$, from which all the kinetic constants can be obtained by curve-fitting.

RESULTS

Activation by Mg^{2+}, Co^{2+} and Mn^{2+}

Effects of these cations on D-xylose isomerase activity were reported by Smith *et al.* (1991) but were re-investigated with the use of carefully reconstituted holoenzymes. Fig. 2 shows the results for both D-xylose and D-fructose isomerase activity at 30 °C at pH 7, with substrate concentrations (100 mM-D-xylose or 1 M-D-fructose) that are well in excess of the observed $K_{m(app.)}$ for the Mg^{2+}-enzyme. Mg^{2+} shows the highest specific activity, with an apparent activation constant of 60–100 μM for both sugars. The apparent activation constant for Co^{2+} was 20 μM but the maximum activity was less than 50% of that with Mg^{2+}, except at Co^{2+} concentrations above 10 mM with fructose as substrate. Mn^{2+} appears to be a poor activator for both fructose (8% of the Mg^{2+} activity) and for xylose (5%) with an apparent activation constant of 10 μM. The true maximum velocity of the Co^{2+}- and Mn^{2+}-enzymes for fructose may be higher, since the $K_{m(app.)}$ for fructose with these cations proved to be surprisingly high (see below). However, for use of the enzyme in isomerization of high-concentration-glucose syrups, Mg^{2+} ions are clearly the most efficient as well as the most food-acceptable activators.

Table 1. Competition between Mg^{2+} and Co^{2+} as activators

The reconstituted Mg^{2+}- and Co^{2+}-holoenzymes were assayed at 30 °C in 0.1 M-Mops buffers, pH 7.90, containing concentrations of D-fructose and bivalent ions as indicated.

[D-Fructose] (M)	[Mg^{2+}] (mM)	[Co^{2+}] (mM)	Activity (μmol/min per mg of enzyme)	
			Mg^{2+}-enzyme	Co^{2+}-enzyme
1.5	10	0	2.0	–
1.5	0	2	–	3.5
1.5	10	2	2.5	3.9
4.0	10	0	1.9	–
4.0	0	2	–	5.3
4.0	10	2	2.8	5.4

Competition between Mg^{2+} and Co^{2+}

Table 1 summarizes assays of the reconstituted Mg^{2+}- or Co^{2+}-enzymes at 30 °C at pH 7.9, with very high D-fructose concen-

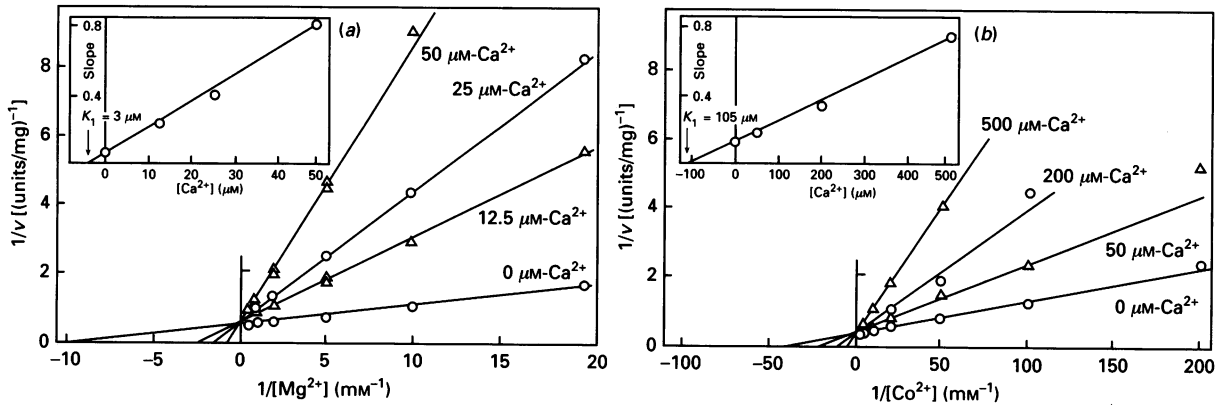

Fig. 3. Inhibition by $[Ca^{2+}]$ of D-fructose isomerase activity

Apoenzyme (0.4 mg/ml) was preincubated at 30 °C for 5 h in the indicated concentrations of Ca^{2+} and (*a*) Mg^{2+} in 0.05 M-Tris/HCl buffer, pH 8.0, or (*b*) Co^{2+} in 0.05 M-Tris/HCl buffer, pH 7.0, and assayed against 1.5 M-D-fructose in similar buffers. The Lineweaver–Burk plots show competitive inhibition by Ca^{2+} of both activator ions and the secondary plots of slope versus $[Ca^{2+}]$ (insets) give the respective inhibition constants (K_i).

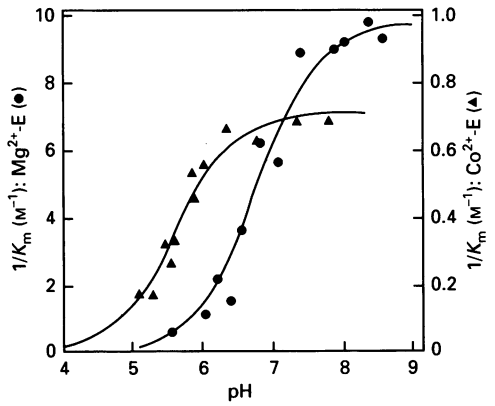

Fig. 4. pH-dependence of K_m for D-fructose of the Mg^{2+}- and Co^{2+}-enzymes

The reconstituted apoenzymes were assayed at 30 °C against 0.04–3 M-D-fructose [S] in 0.1 M buffers (pH 4.60–5.20, acetate; pH 5.50–6.50, Mes; pH 6.75–7.90, Mops; pH 8.1–8.30, Hepes; pH 8.50–9.20, Caps) containing 10 mM-Mg^{2+} (●) or 2 mM-Co^{2+} (▲). Values of K_m were obtained by non-linear-regression analysis on the data as described in the Materials and methods section. The points are fitted to theoretical single-ionization curves for a group with pK_a 6.80±0.07 for the Mg^{2+}-enzyme and 5.6±0.08 for the Co^{2+}-enzyme.

trations (1.5 M and 4 M) in buffers containing saturating concentrations of Mg^{2+} and/or Co^{2+}. The results show that the Co^{2+}-enzyme is more active than the Mg^{2+}-enzyme in 4 M-D-fructose, and that the Co^{2+}-enzyme has a surprisingly higher $K_{m(app.)}$ for this substrate. When both Mg^{2+} and Co^{2+} are present together, the results suggest that neither can quickly displace the previously strongly bound metal ion(s) in the reconstituted holoenzymes.

Inhibition by Ca^{2+}

The inhibition of D-fructose isomerase activity by Ca^{2+} is shown as a Lineweaver–Burk plot for both the Mg^{2+}-enzyme (Fig. 3*a*) and the Co^{2+}-enzyme (Fig. 3*b*). Since the lines intersect on the origin, it is clear that Ca^{2+} competes for the same site(s) in the enzyme as Mg^{2+} or Co^{2+}, and from the slopes of these lines (Fig. 3*a* and 3*b* insets) inhibition constants (K_i) of 3 μM are found for the Mg^{2+}-enzyme and 105 μM for the Co^{2+}-enzyme. The activation constant for Mg^{2+} obtained from these experiments was 100 μM and that for Co^{2+} was 25 μM. It is clear that Ca^{2+} binds with an affinity that is an order of magnitude higher than Mg^{2+} and comparable with that for Co^{2+}.

pH-dependence of K_m of the Mg^{2+}- and Co^{2+}-enzymes

Fig. 4 shows the values of K_m obtained from a series of assays at 30 °C in saturating concentrations of either metal ion (10 mM for Mg^{2+}, 2 mM for Co^{2+}) at various substrate concentrations over a range of pH. Values for Co^{2+} above pH 8 are unreliable because of the limited solubility of the cation. It is clear that $1/K_m$ for fructose with both cations decreases at acid pH and that the theoretical single ionization curves that are fitted to the data by non-linear regression using the ENZFITTER program (Biosoft, Cambridge, U.K.) are for single ionization constants of pK_a 6.80±0.07 for the Mg^{2+}-enzyme and 5.6±0.08 for the Co^{2+}-enzyme.

pH-dependence of maximum velocity of the Mg^{2+}- and Co^{2+}-enzymes

Values of $V_{max.}$ obtained from the above experiments were unreliable, because variable amounts of enzyme had been used over the series of assays. Hence the data shown in Fig. 5 were obtained at 30 °C and similar metal ion concentrations with 3.2 M-D-fructose, which is in large excess of the $K_{m(app.)}$ for the Mg^{2+}-enzyme (0.12 M above pH 7.5) at all pH values higher than 6.70. Values of $V_{max.}$ for the Mg^{2+}-enzyme at lower pH are corrected using the $K_{m(app.)}$ values shown in Fig. 4. For the Co^{2+}-enzyme, all $V_{max.}$ values are so corrected, since $K_{m(app.)}$ increases rapidly below pH 8 from a minimum of 1.6 M. The theoretical curves show that in both cases $V_{max.}$ depends on a single ionizing group with pK_a 6.0±0.07 for the Mg^{2+}-enzyme and 5.3±0.08 for the Co^{2+}-enzyme.

From these two sets of data, values of $V_{max.}/K_m$ can be derived as shown in Fig. 6. The data fit the theoretical curves for a single ionizing group of $pK_a = 7.0 \pm 0.01$ in the Mg^{2+}-enzyme and 5.90±0.05 in the Co^{2+}-enzyme.

Temperature-dependence and pH-dependence of K_m and $V_{max.}$

Because it had become clear that different ionizing groups in the active site were responsible for the pH-dependence of K_m and $V_{max.}$, a series of studies were made with the Mg^{2+}-enzyme at 40.1 °C at various D-fructose concentrations and at various pH values exactly similar to those described above at 30 °C. Linear plots of K_m versus $[H^+]$ (not shown) showed that the pK_a for the

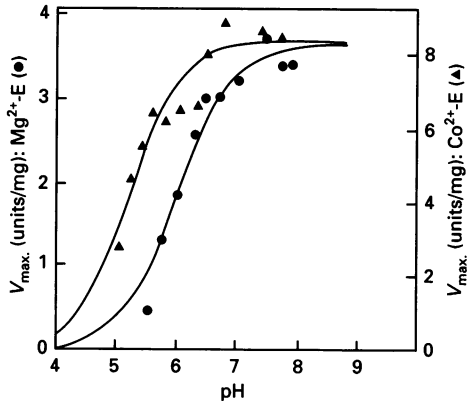

Fig. 5. pH-dependence of $V_{max.}$ for D-fructose of the Mg^{2+}- and Co^{2+}-enzymes

The reconstituted apoenzymes were assayed at 30 °C against 3.2 M-D-fructose in buffers of various pH values, as in Fig. 4, containing 10 mM-Mg^{2+} (●) or 2 mM-Co^{2+} (▲). The apparent values of $V_{max.}$ at various pH values are corrected by using the values of K_m shown in Fig. 3 and fitted to theoretical single-ionization curves for a group of pK_a 6.0±0.07 for the Mg^{2+}-enzyme and 5.3±0.08 for the Co^{2+}-enzyme.

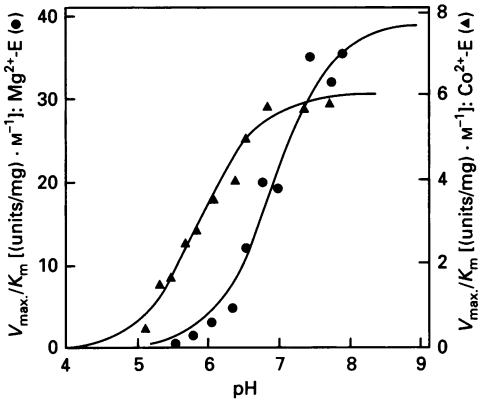

Fig. 6. pH-dependence of $V_{max.}/K_m$ for D-fructose of the Mg^{2+}- and Co^{2+}-enzymes

The data from Figs. 4 and 5 for 10 mM-Mg^{2+} (●) or 2 mM-Co^{2+} (▲) are fitted to theoretical single-ionization curves for a group of pK_a 7.0±0.1 for the Mg^{2+}-enzyme and 5.90±0.05 for the Co^{2+}-enzyme.

group controlling K_m had decreased from 6.80 to 6.65. Assuming a linear Arrhenius plot of pK_a versus $1/T$, an enthalpy of ionization of around 27 kJ/mol (6.5 kcal/mol) can be calculated, which is consistent with the ionization of one of the two active-site histidine residues rather than any of the carboxy groups.

To determine the enthalpy of ionization of the group that controls maximum velocity, assays exactly analogous to those described above (Fig. 5) were made at various temperatures and at various pH values with the Mg^{2+}-enzyme, with 3.2 M-D-fructose as substrate. The results are illustrated in Fig. 7 as an Arrhenius plot of pK_a versus $1/T$, from the slope of which a heat of ionization of 23.5±3 kJ/mol (5.6±0.8 kcal/mol) can be calculated. This is also consistent with the ionization of the imidazole group of a histidine residue.

pH-dependence of K_i for competitive inhibitors

To analyse the catalytic mechanism, it is important to know whether $K_{m(app.)}$ is a true reflection of the substrate dissociation constant (K_s) or a complex constant that includes one or more

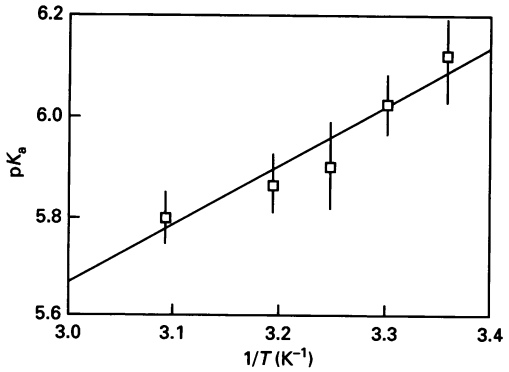

Fig. 7. Temperature-dependence of the pK_a in the Mg^{2+}-enzyme that controls $V_{max.}$

Assays were against 3.2 M-D-fructose in the range of buffers containing 10 mM-Mg^{2+} described in Fig. 5, at temperatures from 20 °C to 50 °C. The apparent $V_{max.}$ values were corrected for variations in $K_{m(app.)}$ and fitted to theoretical titration curves with the pK_a values shown above, which are plotted against the reciprocal of absolute temperature. The slope ($\Delta H/RT$) yields an enthalpy of ionization = 23.5±3 kJ/mol.

kinetic steps. For this purpose, the pH-dependence of the inhibition constant (K_i) for two competitive inhibitors was determined: 5-thio-α-D-glucopyranose has been shown to bind to the active site of this enzyme in a conformation that mimics that of pyranose substrates before the ring-opening step in the mechanism proposed by Collyer *et al.* (1990), whereas D-sorbitol binds in a conformation that mimics the open-chain form first observed by Henrick *et al.* (1989).

Assays were made at 30 °C in 0.1 M buffers (Hepes, pH 7.90, Mops, pH 7.45 or 7.50, and Mes, pH 6.20) containing 0.01 M-Mg^{2+}, with various concentrations of D-fructose as substrate in presence of various concentrations of 5-thio-α-D-glucopyranose (Fig. 8*a*) or D-sorbitol (Figs. 8*b*, 8*c* and 8*d*). In both cases, Lineweaver–Burk plots of $1/v$ versus 1/[D-fructose] showed that the inhibition was strictly competitive, whereas D-sorbitol shows mixed inhibition when assayed against D-xylose (Smith *et al.*, 1991). The results are presented in Fig. 8 as Dixon plots (Dixon & Webb, 1964, pp. 315–359) and clearly show that K_i is invariant with pH over the range studied (pH 6.2–7.9). Since $K_{m(app.)}$ varies with pH, this shows that it must be a complex constant and not a simple dissociation constant.

Order of ligand binding

Since the mechanism proposes binding of substrate plus two metal ions at different sites with different roles, it is important to establish the order of binding of these ligands. The kinetic analysis described by Dixon & Webb (1964, pp. 420–443) allows this for a simple Michaelis–Menten case with one activator plus substrate. In the Materials and methods section, we extend the kinetic analysis to the proposed mechanism to cover a case (Scheme 1) in which both activator ions bind before the substrate can bind, or a case (Scheme 2) in which one activator ion binds first, then substrate, then a second activator ion. These cases can be distinguished by a series of assays at constant activator ion concentration [M] and variable fructose concentration [S] or a series at constant [S] and variable [M].

Order of ligand binding to the Co^{2+}-enzyme

Fig. 9 shows Lineweaver–Burk plots for a series of assays at 30 °C at pH 7.0, at several concentrations of Co^{2+} and various fructose concentrations. The data clearly fit Scheme 1, since the lines intersect on the $1/v$ axis corresponding to a value of k[E] of

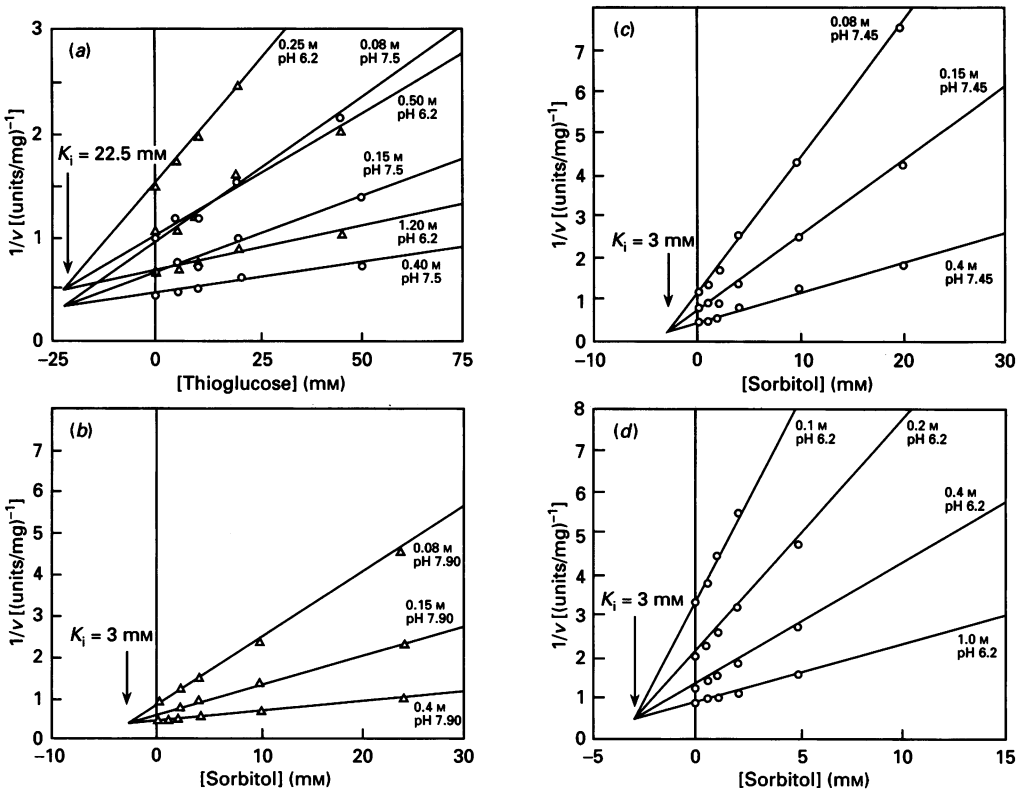

Fig. 8. Competitive inhibition of the Mg^{2+}-enzyme by 5-thio-α-D-glucopyranose or D-sorbitol

A range of D-fructose concentrations in 0.1 M buffers containing 0.01 M-Mg^{2+} (Hepes, pH 7.90; Mops, pH 7.45 or 7.50; Mes, pH 6.20) was assayed at 30 °C in the presence of (*a*) 0–50 mM-5-thio-α-D-glucopyranose, or (*b*), (*c*) and (*d*) 0–25 mM-D-sorbitol. The Dixon plots show competitive inhibition in both cases, yielding values of K_i that are pH-independent.

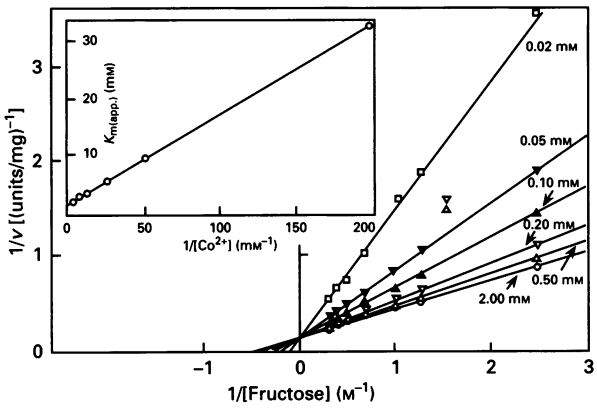

Fig. 9. Lineweaver–Burk plots for D-fructose isomerase activity at various $[Co^{2+}]$ values

Assays were at 30 °C in 0.1 M-Mops buffer, pH 7.0, containing a range of [D-fructose] values and Co^{2+} at the concentrations indicated. $V_{max.}$ is clearly independent of $[Co^{2+}]$. The plot for 0.005 mM-Co^{2+} is not shown. The inset graph, showing values of $K_{m(app.)}$ derived from the intercepts plotted against $1/[Co^{2+}]$, has a slope corresponding to K_1 = 0.1 mM and K_m' = 1.7 M.

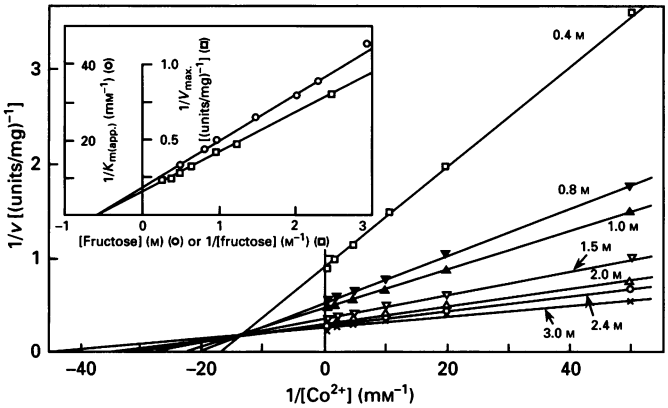

Fig. 10. Lineweaver–Burk plots for isomerase activity (*v*) at fixed [D-fructose] and a range of $[Co^{2+}]$

Assays were at 30 °C in 0.1 M-Mops buffer, pH 7.0. The inset graph, showing derived values of $K_{m(app.)}$ and $V_{max.}$ plotted against [D-fructose] and 1/[D-fructose], corresponds to K_1 = 0.1 mM and K_m' = 1.6 M.

7 units/mg (eqn. 1) and the secondary plot of $K_{m(app.)}$ versus $1/[Co^{2+}]$ (inset) gives a straight line (eqn. 2) that yields values of K_1 = 0.1 mM and K_m = 1.7 M. The value of K_2 appears to be below the lowest concentration of Co^{2+} used in the experiments.

Fig. 10 shows another set of data under similar conditions at several concentrations of fructose and variable $[Co^{2+}]$. The data are plotted according to eqn. (3), and are again consistent with Scheme 1. The secondary plots (inset) of $1/V_{max.}$ versus 1/[S] and of $1/K$ versus [S] are linear and yield values of k[E] = 7 units/mg, K_1 = 0.1 mM and K_m = 1.6 M.

Order of ligand binding to the Mg^{2+}-enzyme

An analogous series of experiments was conducted with Mg^{2+} ions at 30 °C at pH 7.9. At fixed $[Mg^{2+}]$ and variable [D-fructose],

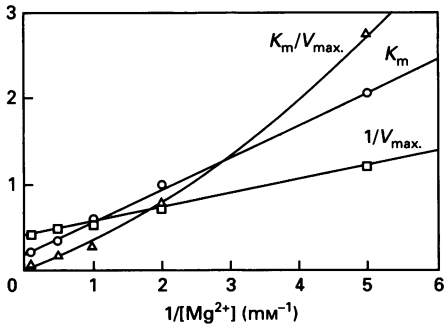

Fig. 11. Apparent $V_{max.}$, K_m and $K_{m(app.)}/V_{max.}$ at fixed [Mg^{2+}] and variable [D-fructose]

Assays were at 30 °C in 0.1 M-Mops buffer, pH 7.90, containing a range of [D-fructose] and Mg^{2+} at the concentrations indicated. Values of apparent $K_{m(app.)}$ and $V_{max.}$ were derived from the slopes and intercepts of $1/v$ plotted against 1/[D-fructose]. The slope of the plot of $1/V_{max.}$ versus 1/[Mg^{2+}] corresponds to $K_{2(app.)} = 0.5$ mM and the slope of the plot of $K_{m(app.)}$ versus 1/[Mg^{2+}] yields $K_m = 0.8$ M. The parabolic plot of $K_{m(app.)}/V_{max.}$ versus 1/[Mg^{2+}] yields $K_1 = 0.2$ mM. Units: $1/V_{max.}$, (units/mg)$^{-1}$; K_m, M; $K_m/V_{max.}$, (M)/units per mg.

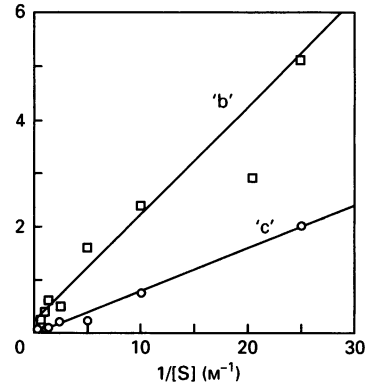

Fig. 12. Apparent $V_{max.}$ and K_m at fixed [D-fructose] and variable [Mg^{2+}]

Assays were at 30 °C in 0.1 M-Mops buffer, pH 7.90, containing a range of [Mg^{2+}] and D-fructose (S) at the concentrations indicated. The values of 'b' [(mM)/units per mg] and 'c' [(mM)^2 (M^{-1})/units per mg] indicated are derived from fitting the observed rates (v) to equations for parabolas:

$$1/v = a + b(1/[M]) + c(1/[M])^2$$

and yield values for $K_1 = 0.3$ mM, $K_{2(app.)} = 0.7$ mM and $K_m = 0.7$ M.

the Lineweaver–Burk plots were linear (not shown). However, the values of apparent $V_{max.}$ and $K_{m(app.)}$ derived by non-linear-regression analysis of the data (ENZFITTER Data Analysis Program) fit Scheme 2 rather than Scheme 1 since $1/V_{max.}$ and $K_{m(app.)}$ vary with metal ion concentration, as can be seen from the secondary plots fitted by least-squares analysis, shown in Fig. 11. The secondary plot of $K_{m(app.)}/V_{max.}$ versus 1/[Mg^{2+}] is parabolic (Cricket Graph 1.3; Cricket Software, Malvern, PA, U.S.A.). Eqns. (5), (6) and (7) yield values of $k[E] = 2.4$ units/mg, $K_2(1+K_O) = K_{2(app.)} = 0.5$ mM, $K_m = 0.8$ M and $K_1 = 0.2$ mM.

A parallel set of experiments in which [Mg^{2+}] was varied at a set of fixed [D-fructose] confirms that the Mg^{2+}-enzyme fits Scheme 2 rather than Scheme 1. Plots of $1/v$ versus 1/[Mg^{2+}] were parabolic using the Cricket Graph Version 1.3 ($y = a + bx + cx^2$) as predicted from eqn. (8) (not shown). In Fig. 12 the values of $b\{K_2(1+K_O)\ ([S]+K_m)/k[E][S]\}$ and $c\,(K_1K_2K_FK_O/k[E][S])$ from the parabolic curves fitted to this data are plotted against 1/[S] according to eqn. (8). From least-squares fits of plots of b and c versus 1/[S], all the constants can be calculated. The b plot has intercept $K_2(1+K_O)/k[E] = 0.29$ and slope $K_2(1+K_O)K_m/k[E] = 0.20$, yielding $K_{2(app.)} = 0.7$ mM

Table 2. Kinetic constants for *Arthrobacter* B3728 D-fructose isomerase activity at 30 °C

The kinetic constants are calculated from Schemes 1 or 2 as appropriate and unless otherwise stated are corrected for ionization of active-site histidine residues. Abbreviation: N.D., not determined. – indicates does not apply.

Substrate	[M^{2+}]	K_1 (mM)	K_2' (mM)	K_2 (mM)	K_m (M)	K_m' M)	k (s^{-1})	pK_a (±0.1) controlling K_m (ΔH)	pK_a (±0.1) controlling $k(\Delta H)$	pK_a (±0.1) controlling k/K_m
D-Fructose	Mg^{2+} (1–10 mM)	0.2	–	0.5	0.8	–	2.1	6.8 (27 kJ/mol)	6.0 (23.5 kJ/mol)	7.0
D-Fructose	Mg^{2+} (10–400 mM)	N.D.	2	–	–	0.11	2.1	6.2	5.2	6.3
D-Fructose	Co^{2+} (0.005–2 mM)	0.1	–	< 0.005	–	1.7	6.5	5.6	5.3	5.9
D-Fructose	Mn^{2+} (10 mM)	N.D.	N.D.	N.D.	–	N.D.	0.2*	N.D.	N.D.	–
D-Glucose**	Mg^{2+} (30 mM)	–	–	–	–	0.23	2.3	N.D.	N.D.	–
D-Xylose**	Mg^{2+} (30 mM)	–	–	–	–	0.0033	8.9	–	–	–

Substrate	[M^{2+}]	Inhibitor	K_i (mM)
D-Fructose (1.5 M)	Mg^{2+} (0.05–50 mM)	Ca^{2+} (0.0125–0.05 mM)	0.003
D-Fructose (3.0 M)	Co^{2+} (0.005–2 mM)	Ca^{2+} (0.05–0.5 mM)	0.105
D-Fructose (0.08–0.4 M)	Mg^{2+} (10 mM)	5-Thio-α-D-glucopyranose (0–50 mM)	22.5
D-Fructose (0.08–1.2 M)	Mg^{2+} (10 mM)	D-Sorbitol (0–25 mM)	3
D-Fructose (0.08–1.2 M)	Mg^{2+} (400 mM)	D-Sorbitol (0–25 mM)	3
D-Fructose (0.08–1.2 M)	Co^{2+} (2 mM)	D-Sorbitol (0–25 mM)	60
D-Xylose (0–15 mM)†	Mg^{2+} (30 mM)	D-Sorbitol (0–15 mM)	6.5
D-Xylose (0–15 mM)†	Mg^{2+} (30 mM)	D-Xylitol (0–0.5 mM)	0.3

* Assays with 1 M-D-fructose, pH 7.
† pH 8.0; data from Smith *et al.* (1991).

and $K_m = 0.7$ M. As expected, the plot of c versus $1/[S]$ passes through the origin, and the slope $\{K_1K_2(1+K_O)K_m/k[E] = 0.08\}$ yields $K_1 = 0.3$ mM.

Measurements of kinetic parameters at very high Mg^{2+} concentrations

Although these results show that in the range 0.1–10 mM the second Mg^{2+} ion binds only after ring-opening and chain extension, it appeared possible that at very high $[Mg^{2+}]$ both sites in the enzyme might become saturated before substrate was bound. Hence an analogous study was made of activity at 30 °C versus various [fructose] at several different pH values, but with 400 mM-Mg^{2+} rather than 10 mM-Mg^{2+}. This allowed calculation of $K_{m(app.)}$ and $V_{max.}$ at each pH (results not shown). Within experimental error, there was no significant change in the values for $K_{m(app.)}$ (0.11 M versus 0.12 M) and $V_{max.}$ for the high-pH form of the enzyme (3.15 versus 3.3 units/mg), but the pK_a of the group controlling $V_{max.}$ fell from 6.0 ± 0.07 to 5.2 ± 0.1, and the pK_a for the group controlling $K_{m(app.)}$ fell from 6.80 ± 0.07 to 6.2 ± 0.1.

To exclude the possibility that this difference was due to a general salt effect, analogous experiments were conducted in the presence of 10 mM-Mg^{2+} plus 1.17 M-NaCl. Within experimental error (results not shown) both the absolute values for $K_{(m(app.)}$ (0.12 M) and $V_{max.}$ (3.3 units/mg) and the pK_a controlling $V_{max.}$ (6.0) and $K_{m(app.)}$ (6.8) were the same as in the presence of 10 mM-Mg^{2+} alone (see Table 2).

DISCUSSION

Metal ion affinity and enzyme activity

The crystallographic studies by Collyer *et al.* (1990) clearly show that in the presence or the absence of xylose, Mn^{2+} or Co^{2+} ions bind at both Site 1 and Site 2, whereas Mg^{2+} is seen only at Site 1. There is other evidence for two bivalent metal ion sites in the active sites of analogous D-xylose isomerases. By equilibrium dialysis and spectral displacement, Callens *et al.* (1988) showed two different Co^{2+} sites per monomer in D-xylose isomerase from *Streptomyces violaceoruber*. The high-affinity site (dissociation constant $K_d < 0.3$ μM) appeared to have six-co-ordinate octahedral symmetry. The weaker Co^{2+} site ($K_d = 25$ μM) corresponds to the activation constant found in earlier studies and appeared to be either four- or five-co-ordinate (Callens *et al.*, 1985, 1986, 1988). With Mg^{2+}, only a single binding constant was seen ($K_d = 10$ μM), but the activation constant had $K_d = 417$ μM so that two sites are again indicated. Octahedral co-ordination of Co^{2+} at the high-affinity site, with one ligand being an imidazole ring nitrogen atom, was also observed in an X-ray-absorption study of D-xylose isomerase from *Streptomyces albus* (Nolting *et al.*, 1989).

pH-dependence and temperature-dependence of K_m and K_i

Collyer *et al.* (1990) suggested that the rate-limiting step is ring-opening, but we conclude that it is the isomerization step. One argument is available from the crystallographic data alone. If the rate-limiting step were to be ring-opening, the substrate should be seen in the pyranose form in crystals soaked in D-xylose. This ring form is seen in crystals soaked in 5-thio-α-D-glucose, which cannot ring-open. In contrast, D-xylose is seen in the Mn^{2+}-enzyme as the extended open-chain form with Mn^{2+} at Sites 1 and 2, not 2′. This suggests that the rate-limiting step lies after ring-opening and chain extension.

The effects of pH and temperature on K_m and K_i are consistent with this view. Table 2 summarizes the kinetic constants determined from Scheme 1 for the Co^{2+}-enzyme and Scheme 2 for the Mg^{2+}-enzyme. If ring-opening were the rate-limiting step, K_m would be a simple binding constant analogous to K_i for competitive inhibitors. However Table 2 shows that K_m is pH-dependent whereas K_i values for both sorbitol and 5-thio-α-D-glucopyranose are absolutely independent of pH. These K_i values represent true binding constants, since tertiary structures of the enzyme–metal ion–inhibitor complexes are available (Henrick *et al.*, 1989; Collyer *et al.*, 1990). Hence K_m should also be pH-independent if ring-opening were rate-limiting. Table 2 shows that it has a pK_a and heat of ionization consistent with those for a histidine residue.

However, if the pathways are as summarized in Scheme 3, where isomerization at Site 2 is the rate-limiting step (k), K_m becomes a complex constant that includes the fructose dissociation constant (K_F or K_F') and the equilibrium constant between extended and ring-chain forms (K_O and K_O'):

$$K_m = \frac{K_F'K_O'}{(1+K_O')}$$

K_O and K_O' represent the ratio of the slowest reverse and slowest forward rates in the ring-opening and chain-extension steps (k_O, k_{-O}, k_E and k_{-E} for Mg^{2+} or k_O', k_{-O}', k_E' and k_{-E}' for Co^{2+}). It is likely that $k_E > k_{-E}$, since the substrate is seen in crystals in the extended form and not in the pseudo-cyclic form; this implies that O-2/O-4 co-ordination in the extended chain is more stable than O-2/O-3 co-ordination in a pseudo-cyclic form. It is also likely that $k_{-O} > k_O$, since in solution the rates of ring-closing are very much faster than ring-opening (mutarotation rate constants for α-D-glucopyranose and α-D-fructofuranose at 20 °C are 1×10^{-4} s^{-1} and 9×10^{-4} s^{-1} respectively; Pigman & Isbell, 1968). Hence K_O will be k_{-E}/k_O. There is no reason why k_E or k_{-E} should be pH-dependent, whereas k_O will reduce and K_O will increase when His-53 ionizes. This explains the pH-dependence of K_m, since we have shown above that K_F will be pH-independent.

pH-dependence of maximum velocity

This reflects ionization of a histidine residue; it must be unprotonated to allow binding of M^{2+} at Site 2, and hence isomerization. Table 2 shows that the apparent pK_a that controls the catalytic rate constant (k) is much lower for the Co^{2+}-enzyme that for the Mg^{2+}-enzyme. Co^{2+} is more strongly bound than Mg^{2+}; hence a higher concentration of H^+ ions is needed to displace it.

The apparent pK_a of the group that controls $V_{max.}$ and the high heat of ionization derived from the Arrhenius plots shown in Fig. 7 are consistent with a histidine residue rather than a carboxy group or amino group, which have much lower or higher temperature coefficients respectively. The only plausible candidate at Site 2 is His-219. This is important for the industrially important aim of lowering the pH optimum of a glucose isomerase, since it means that increased activity at low pH arises automatically from operation at high temperatures.

The steady-state kinetics says nothing about the postulated hydride-shift mechanism for isomerization, but recent experiments on the effects of ^2H_2O support this, and also confirm that isomerization is the rate-limiting step (Lee *et al.*, 1990).

Order of ligand binding

There is abundant evidence with similar enzymes that substrates and inhibitors bind to D-xylose isomerases only when there is a metal cation at Site 1, e.g. n.m.r. studies (Young *et al.*, 1975; Bock *et al.*, 1983) or protection against chemical modification of His-53 (Vangrysperre *et al.*, 1988, 1990). Since Co^{2+} and Mn^{2+} bind most strongly at Site 2, the activation constants found with the *Arthrobacter* enzyme for Co^{2+} ($K_d = 20$ μM) and

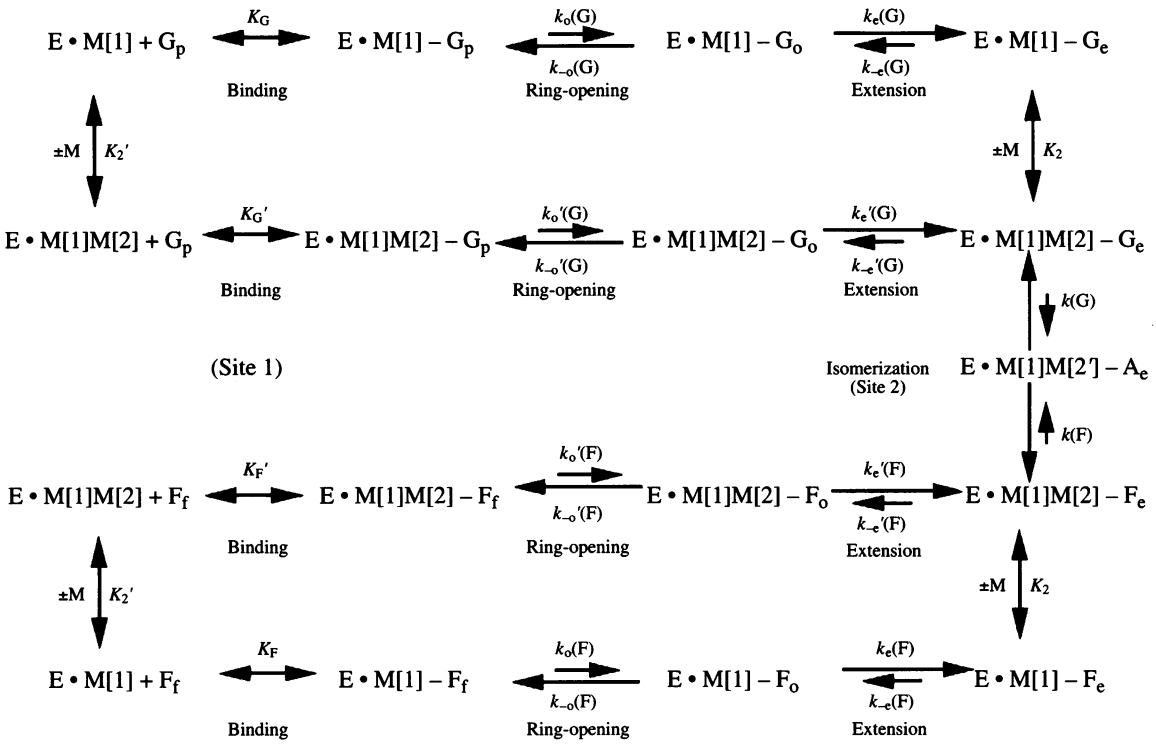

Scheme 3. Summary of the proposed catalytic mechanisms

Key: G_p, α-D-glucopyranose; G_o, glucose open-chain aldehyde, pseudo-cyclic form; G_e, glucose open-chain aldehyde, extended form; A_e, extended open-chain ionic form; F_f, α-D-fructofuranose; F_o, fructose open-chain ketone, pseudo-cyclic form; F_e, = fructose open-chain ketone, extended form.

Mn^{2+} (10 μM) must correspond to binding at Site 1 and the kinetic pathway shown as Scheme 1 will apply.

However Mg^{2+} binds most strongly to Site 1, so the pathway shown as Scheme 2 was a possibility. For this reason, we compared in detail the dependence of rate on the concentrations of both D-fructose and Mg^{2+} or Co^{2+}. For both Mg^{2+} and Co^{2+}, the $K_{m(app.)}$ for fructose is dependent on $[M^{2+}]$. This indicates that fructose cannot bind to the apoenzyme, but only to the enzyme–M^{2+} complex as predicted from the crystallographic results.

With Co^{2+}, the results shown that two metal ions bind before the substrate binds, as assumed in the mechanism proposed by Collyer *et al.* (1990). At various concentrations of fructose (Fig. 9), $V_{max.}$ is invariant with $[Co^{2+}]$ and $K_{m(app.)}$ varies proportionally to 1/[M] as predicted from Scheme 1 (eqns. 2 and 3). At various values of $[Co^{2+}]$ (Fig. 10), $V_{max.}$ varies inversely to and K varies proportionally to the concentration of fructose (eqn. 3).

However, below 10 mM-Mg^{2+}, the order of binding is Mg^{2+} at Site 1, then substrate at Site 1, then Mg^{2+} at Site 2, as predicted by Scheme 2. At various fructose concentrations, $1/V_{max.}$ is proportional to $1/[Mg^{2+}]$ (Fig. 11), giving $K_{2(app.)} = 0.5$ mM, as predicted from eqn. (5), and eqn. 6 is also obeyed, giving $K_m = 0.8$ M for E·Mg[1].

At very high concentrations of Mg^{2+} between 10 mM and 400 mM, both Site 1 and Site 2 are occupied before substrate binds, so the kinetics fit Scheme 1, as for Co^{2+}. These results give $K_m' = 0.11$ M for the E·Mg[1]·Mg[2] form, and K_2' (the dissociation constant from Site 2 in the free enzyme) = 4 mM. This conclusion is supported by Fig. 11, where the plot of $K_{m(app.)}$ cuts the 1/[M] axis at around 0.5 mM^{-1}, corresponding to $K_2' = 2$ mM, rather than passing through the origin as predicted from eqn. (6). This confirms that the second metal ion binds strongly to Site 2 ($K_{2(app.)} = 0.5$ mM) only when fructose is present.

The inhibition constants (K_i) for Ca^{2+}, 3 μM for the Mg^{2+}-enzyme and 105 μM for the Co^{2+}-enzyme refer to the binding constants for Site 2 and Site 1 respectively.

Substrate-specificity

The kinetic studies were with D-fructose because the assay techniques are more convenient, although D-xylose is the natural substrate and D-glucose is the commercial substrate. Table 2 shows that with Mg^{2+}, the isomerization rate (k) is similar for fructose and glucose and about 25% of that for xylose; this suggests minimal steric hindrance from the 6-CH_2OH group in the transition state. With Co^{2+}, k for fructose is about 3 times higher, showing that this ion is preferred in the transition state.

However, if we use K_m as a measure of substrate-specificity, there is a huge apparent difference between these substrates. Much of this can be explained by the relative abundance of the α-anomers in solution: the n.m.r. studies by Makkee *et al.* (1984) show that these are the preferred forms. The abundance is α-D-xylopyranose 36.5%, α-D-glucopyranose 38% and α-D-fructofuranose 6.5% (Angyal, 1984). Correcting the apparent K_m values shown in Table 2 for this abundance yields values of K_m for α-D-xylopyranose = 1.2 mM, α-D-glucopyranose = 87 mM and α-D-fructofuranose = 52 mM at low Mg^{2+} or 7.2 mM at high Mg^{2+} or 110 mM with Co^{2+}. Allowing that K_m is a complex constant, these values compare with K_i values shown in Table 2 for 5-thio-α-D-glucopyranose. For D-sorbitol, which is an analogue of the open-chain hexoses, K_i is much lower (3 mM) with the Mg^{2+}-enzyme than the Co^{2+}-enzyme (60 mM). These values point to a greater degree of steric hindrance from the 6-CH_2OH group, which lies close to His-53 in the binding and ring-opening steps, than in the isomerization step. The 15-fold difference between high Mg^{2+} and Co^{2+} in K_m for α-D-fructofuranose probably reflects the larger size of the latter, which may reduce flexibility during ring-opening.

If we use $k_{cat.}/K_m$ as a measure of substrate-specificity, the corrected values are α-D-xylopyranose = 742 $M^{-1} \cdot s^{-1}$, α-D-glucopyranose = 26 $M^{-1} \cdot s^{-1}$ and α-D-fructofuranose = 40 $M^{-1} \cdot s^{-1}$ at low Mg^{2+} concentration or 292 $M^{-1} \cdot s^{-1}$ at high Mg^{2+} concentration or 59 $M^{-1} \cdot s^{-1}$ with Co^{2+}.

The research was funded by the Science and Engineering Research Council Protein Engineering Initiative of the U.K.

REFERENCES

Angyal, S. J. (1984) Adv. Carbohydr. Chem. Biochem. **42**, 15–68
Blow, D. M., Birktoft, J. J. & Hartley, B. S. (1969) Nature (London) **221**, 337–340
Bock, K., Meldal, M., Meyer, B. & Wiebe, L. (1983) Acta Chem. Scand. Ser. B **37**, 101–108
Callens, M., Kersters-Hilderson, H., van Opstal, O. & De Bruyne, C. K. (1985) Arch Int. Physiol. Biochim. **93**, B10–B11
Callens, M., Kersters-Hilderson, H., van Opstal, O. & De Bruyne, C. K. (1986) Enzyme Microb. Technol. **8**, 696–700
Callens, M., Tomme, P., Kersters-Hilderson, H., Cornelius, R., Vangrysperre, W. & De Bruyne, C. K. (1988) Biochem. J. **250**, 285–290
Collyer, C. A., Henrick, K. & Blow, D. M. (1990) J. Mol. Biol. **212**, 211–235
Danno, G. (1970) Agric. Biol. Chem. **35**, 997–1006
Dixon, M. & Webb, E. C. (1964) The Enzymes, 2nd edn., Longman Group, Harlow
Duke, F. R., Weibel, M., Page, D. S., Bulgrin, V. G. & Luthy, J. (1969) J. Am. Chem. Soc. **91**, 3904–3909
Good, N. E., Winget, G. D., Winter, W., Connolly, T. N., Izawa, S. & Singh, R. M. M. (1966) Biochemistry **5**, 467–477
Henrick, K., Collyer, C. A. & Blow, D. M. (1989) J. Mol. Biol. **208**, 129–157
Isbell, H. S. & Pigman, W. (1969) Adv. Carbohydr. Chem. **24**, 13–65
Lee, C., Bagdasarian, M., Meng, M. & Zeikus, J. G. (1990) J. Biol. Chem. **265**, 19082–19090
Loviny-Anderton, T. L. F., Shaw, P.-C., Shin, M.-K. & Harley, B. S. (1991) Biochem. J. **277**, 263–271
Makkee, M., Kieboom, A. P. G. & van Bekkum, H. (1984) Recl. Trav. Chim. Pays-Bas **103**, 361–364
Nolting, H.-F., Eggers, P., Henkel, G., Krebs, B., Hemker, J., Witzel, H. & Hermes, C. (1989) Physica B (Amsterdam) **158**, 123–125
Pigman, W. & Isbell, H. S. (1968) Adv. Carbohydr. Chem. **23**, 10–57
Smith, C. A., Rangarajan, M. & Hartley, B. S. (1991) Biochem. J. **277**, 255–261
Vangrysperre, W., Callens, M., Kersters-Hilderson, H. & De Bruyne, C. K. (1988) Biochem. J. **250**, 153–160
Vangrysperre, W., Van Damme, J., Vandekerckhove, J., De Bruyne, C. K., Cornelius, R. & Kersters-Hilderson, H. (1990) Biochem. J. **265**, 699–705
Young, J. M., Schray, K. J. & Mildvan, A. S. (1975) J. Biol. Chem. **250**, 9021–9027

Received 23 May 1991/2 September 1991; accepted 10 September 1991